


Original article

Numerical Modeling of Coastal Upwellings off the Southern Coast of Crimea in Spring-Summer Period, 2010

D. A. Yarovaya , V. V. Efimov

Marine Hydrophysical Institute of RAS, Sevastopol, Russian Federation

 darik777mhi-ras@mail.ru

Abstract

Purpose. The aim of this work is to investigate real cases of upwelling observed off the southern coast of Crimea in late May 2010 using a coupled mesoscale model.

Methods and Results. The coupled mesoscale ocean-atmosphere model NEMO-OASIS-WRF (NOW) with a 1 km resolution was used. The three areas of reduced sea surface temperature observed in satellite images near Yalta, near Feodosia, and in the Kerch Strait in late May 2010 were reproduced. It was found that at a depth of 10 m, the decrease in water temperature was not limited to these three areas, but also took place along the whole coast from Sevastopol to Kerch. The modeling results made it possible to examine in detail two upwelling events, namely those in the Yalta and Feodosia areas. The main advantage of dynamic regionalization in coupled modeling has been demonstrated: the atmospheric block of the coupled model reproduces the fine-scale structure of the surface wind field in the Yalta area, in particular, the intensification of coastal wind over the sea up to significant values of 12–15 m/s, which is absent in the atmospheric reanalysis data.

Conclusions. It is established that the coastal upwelling near Yalta can be classified as wind-driven, as its development was accompanied by an offshore wind. The Feodosia upwelling is of the Ekman type and is caused by the southwesterly alongshore winds. The vertical structure of both upwelling events on cross sections normal to the coastline is shown. The revealed main difference in the upwelling structures is as follows: in the Yalta upwelling, the water uplift was concentrated in a narrower zone directly adjacent to the coast, whereas in the Feodosia upwelling, the main water uplift took place at some distance from the coast, and the uplift velocity did not reach such high values as in the Yalta case. It is shown that the SST decrease near Yalta and Feodosia occurred precisely due to upwelling, as a decrease in surface water temperature was accompanied by a simultaneous increase in salinity and coincided in time with the intensification of the corresponding coastal wind velocity component directed normal to the coast in the Yalta area and parallel to the coast in the Feodosia region. The obtained results have demonstrated that the application of a modern ocean-atmosphere model in mesoscale modeling makes it possible to reproduce and examine in detail the structure and development of real upwelling events near the southern coast of Crimea, which would be impossible using only observational data.

Keywords: mesoscale coupled modeling, Black Sea upwellings, southern coast of Crimea

Acknowledgments: The study was carried out within the framework of the state-funded research theme of FSBSI FRC MHI, project No. FNNN-2024-0014.

For citation: Yarovaya, D.A. and Efimov, V.V., 2026. Numerical Modeling of Coastal Upwellings off the Southern Coast of Crimea in Spring-Summer Period, 2010. *Physical Oceanography*, 33(2), pp. 339-351.

© 2026, D. A. Yarovaya, V. V. Efimov

© 2026, Physical Oceanography



Introduction

A widespread type of coastal upwelling can be explained within the simple Ekman model: in a sufficiently deep sea (depth exceeding the Ekman layer thickness), alongshore wind causes Ekman transport of water from the coast to the sea and, as a consequence, water uplift near the coast. In addition to the Ekman type, wind-driven upwelling caused by wind directed from land to sea can also be observed¹ [1]. In the open sea, upwelling can be associated with large positive vorticity of the surface wind. Such upwelling developed, for example, in the southwestern part of the Black Sea under an abnormally intense mesoscale cyclone on September 25–29, 2005. In this cyclone, the surface wind vorticity reached (1–2) 10^{-3} 1/s, which caused water from a depth of ~ 30 m to rise to the surface [2, 3].

It is known that the appearance of upwelling may not be directly related to the action of surface winds. Another important reason is the dynamics of sea currents, e.g., changes in the speed and direction of alongshore jet currents and the penetration of meanders of the Black Sea Rim Current (RC) into the coastal zone [4].

Climatological studies of coastal upwelling in the Black Sea based on *in situ* and remote sensing data have been carried out repeatedly [4–12]. It was found that a strong coastal wind of favorable direction does not always lead to the rise of cold deep waters to the surface. For example, in [11], two cases of so-called incomplete upwelling off the southern coast of Crimea in June 2013 were reported, when the rise of cold deep waters did not reach the sea surface and did not manifest itself in the sea surface temperature (SST) field. The intensity of upwelling is influenced by the vertical thermal structure of the upper sea layer during a particular period. For instance, according to long-term measurements in the Kalamitsky Gulf and at coastal stations on the southern coast of Crimea, it was found that upwelling in these areas is most frequently observed in June and July, when the vertical temperature gradient in the upper 20 m layer reaches its highest values [5, 6, 9]. It was found that advection of waters from the upwelling area can cause cold SST anomalies in neighboring areas. Reference [9] describes a case of a significant (more than 7 °C per day) SST drop near Yevpatoria on July 17, 2008, which occurred as a result of horizontal transport of cold waters from the northwest, from the Tarkhankut area, where intense upwelling developed under a strong westerly wind. In [13], the mechanism of SST decrease in the southern part of the Karkinitzky Gulf due to advection of colder upwelling waters from the northern part of the gulf was described.

A number of works have been devoted to the study of upwelling using numerical modeling [13–16]. However, these works used either simplified models of ocean

¹ Arkhipkin, V.S., Eremeev, V.N. and Ivanov, V.A., 1987. [*Upwelling in the Marginal Zones of the Ocean*]. Sevastopol: MHI, 46 p. (Preprint/MHI) (in Russian).

circulation (e.g., applying the “rigid lid” approximation at the sea surface) or climatological temperature and salinity fields as initial conditions.

It is worth noting that the width of the coastal upwelling zone in the Black Sea is about 6 km, which corresponds to the characteristic value of the local baroclinic Rossby radius of deformation near the coast [4]. Thus, the study of this small-scale phenomenon requires increased spatial resolution in the model. In our previous work [17], using the example of the episode of September 24–25, 2013, it was shown that the coupled mesoscale model NOW with a 1 km resolution is capable of reproducing upwelling near the southern coast of Crimea.

The aim of this work is to study real cases of upwelling observed off the Crimean coast using a modern tool – the coupled mesoscale ocean-atmosphere model.

Model description

The coupled mesoscale ocean-atmosphere model NEMO-OASIS-WRF (NOW) [18] consists of the NEMO ocean model [19], the WRF atmospheric model², and the OASIS coupler [20], a software package that provides data exchange between the models.

Two nested computational grids with resolutions of 3 and 1 km were used in the simulation. The grid with a 3 km spacing covered the Black and Azov Seas, whereas the grid with a 1 km spacing covered the Crimean Peninsula region (32–40°E, 43.6–47.7°N). The horizontal grids in NEMO and WRF were identical to avoid spatial interpolation during data exchange, which increases computational costs. The atmospheric model used 38 vertical levels, whereas the ocean model used 75 levels, with 42 levels concentrated in the upper 100 m layer.

The simulation was started on May 1, 2010, and lasted for two months. Since the calculation was short-term, the ocean model did not account for river runoff or water exchange with the Marmara Sea (a solid lateral boundary was used in the Bosphorus Strait).

ERA5 reanalysis data were used as initial and lateral boundary conditions for the atmospheric model. Initial conditions for the ocean model were taken from the Copernicus reanalysis data. Ocean surface boundary conditions in the ocean model were specified using atmospheric model data. During the coupled simulation, the following fields were transferred from WRF to NEMO via the OASIS coupler: wind stress at the surface, sensible and latent heat fluxes, surface radiative heat fluxes (shortwave and longwave), and the difference between evaporation and precipitation. From NEMO to WRF, the fields of sea surface temperature and surface current velocity were transferred.

Let us note the main advantage of coupled modeling over the standard approach using only an ocean model. In the coupled NOW model, the fields used as surface boundary conditions for the ocean model are obtained through the so-called dynamic regionalization (downscaling). The mesoscale atmospheric model downscales global reanalysis data for a limited area onto a finer grid with a resolution of several kilometers, taking into account small-scale heterogeneities of the underlying surface

² Skamarock, W.C., Klemp, J.B., Dudhia, J., Gill, D.O., Barker, D.M., Duda, M.G., Huang, X.-Y., Wang, W. and Powers, J.G., 2008. *A Description of the Advanced Research WRF Version 3*. NCAR Technical Note NCAR/TN-475+STR. USA, Colorado, Boulder: National Center for Atmospheric Research, 113 p.

(topography, land use type, vegetation cover) and coastline indentation. As will be shown below, this makes it possible to obtain more detailed information about atmospheric fields that is unavailable in the original reanalysis data.

Modeling results and discussion

Fig. 1, *a* shows the SST field for May 25, 2010 according to satellite observations³. Three areas with reduced SST are clearly distinguished off the Crimean coast: near Yalta, near Feodosia, and in the Kerch Strait. In these areas, SST is $\sim 11\text{--}12\text{ }^{\circ}\text{C}$, which is $3\text{--}4\text{ }^{\circ}\text{C}$ lower than the temperature of the surrounding waters. Without providing illustrations, we note that these cold anomalies began to form in the SST fields on May 22–23 and were observed in satellite images until May 26–27. Figs. 1, *b*, *c* show the temperature fields obtained from coupled modeling for a time close to that shown in Fig. 1, *a*.

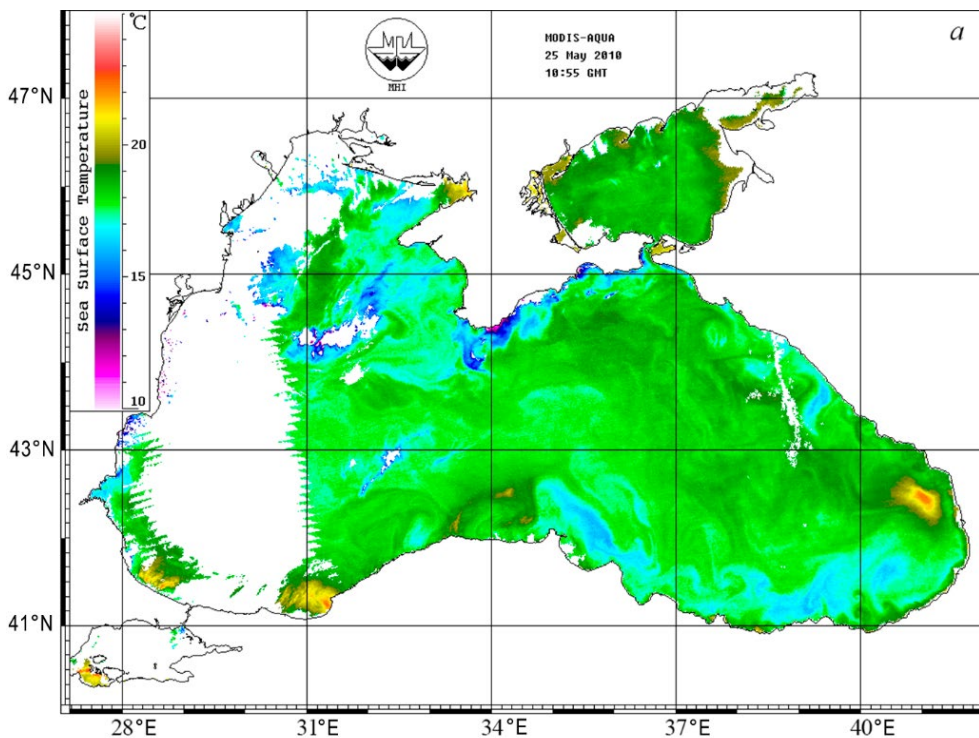


Fig. 1. Sea surface temperature ($^{\circ}\text{C}$) on May 25, 2010: *a* – satellite data, *b* – the NOW model; *c* – water temperature ($^{\circ}\text{C}$) at a depth of 10 m based on the NOW model. Isolines show bottom topography (m), black arrows – near-surface wind velocity, white arrows – surface current velocity; black rectangles highlight the areas shown in greater detail in Fig. 2; black lines inside the rectangles indicate the sections shown in Fig. 3

³ Marine Hydrophysical Institute of RAS. *Marine Portal*. [online] Available at: <http://dvs.net.ru/mp/data/modis/1005/100525bt.gif> [Accessed: 24 March 2026].

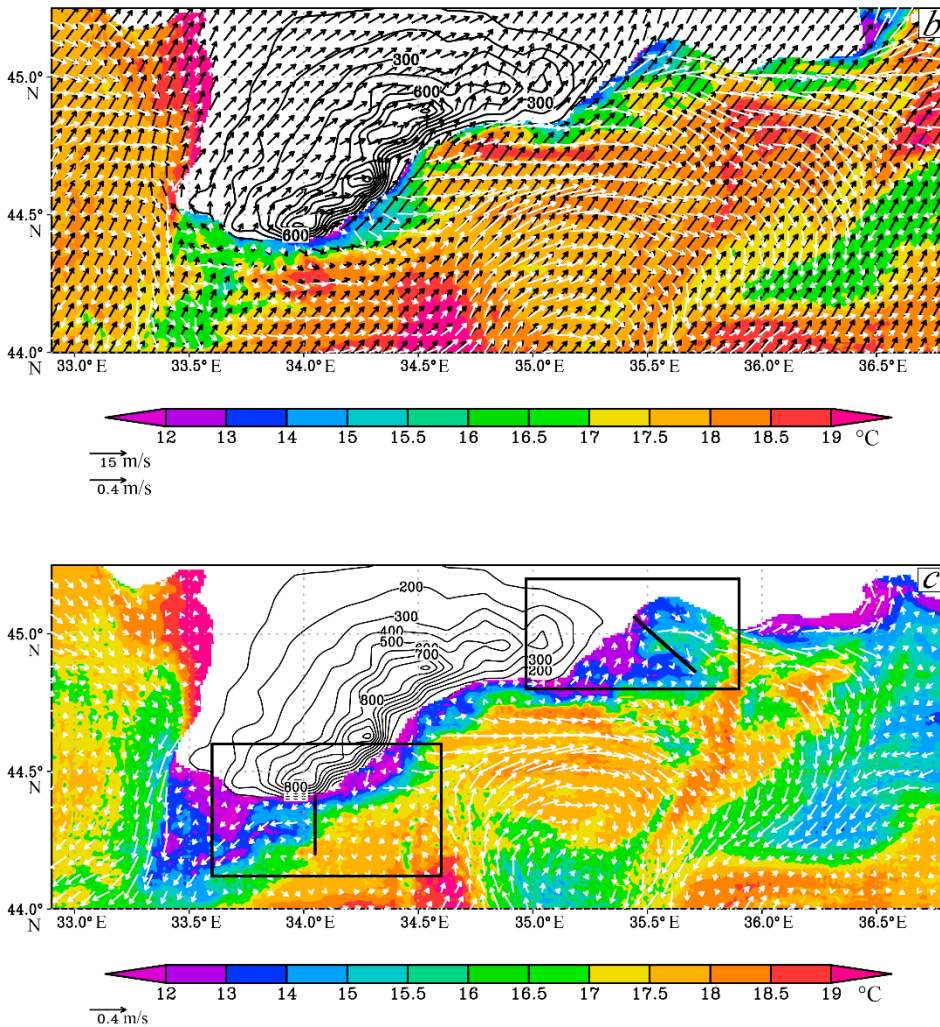


Fig. 1, *b* shows that the model successfully reproduced the appearance of cold SST anomalies near the Crimean coast. It is important to emphasize that these cold anomalies were absent in the initial conditions for the ocean model (as of May 1, 2010); they appeared on May 24–25 as a response of the upper sea layer to the corresponding wind forcing. In Fig. 1, *a, b*, an extended “tongue” of reduced (by $\sim 2\text{--}3$ °C) SST directed from the southern tip of the peninsula to the south is also visible. This likely resulted from horizontal advection of cold waters from the Yalta upwelling. Such advection can be caused by coastal eddies occurring on the periphery of the RC, which capture cold upwelling waters and, moving together with the RC, transport them southwestward into the open sea [10].

Furthermore, in Fig. 1, *a, b*, it can be seen that the NEMO model reproduced elevated SST values in the Kalamitsky Gulf, where the water temperature is 19 °C, which is ~1–2 °C higher than in the adjacent area. The Kalamitsky Gulf is shallow; its depth decreases from ~30 m at the outer part of the gulf to ~15 m near the coast. This obviously contributes to rapid warming of the entire water column in the gulf during the seasonal increase in atmospheric heat fluxes.

In addition to the SST field, Fig. 1, *b* shows the fields of surface current and surface wind speed. In the current field, water outflow from the coast is clearly visible near Yalta, where the current is directed southeastward, normal to the coast, and near Feodosia, where the current velocity is directed predominantly eastward. These features of the current velocity field will be discussed in more detail below. Moreover, in the current fields (Fig. 1, *b, c*), the Yalta anticyclonic eddy southeast of Crimea with its center at 35.2°E, 44°N is well expressed; it is part of the general circulation of the Black Sea waters (the northern half of the eddy is visible in the figures). In the wind field, it can be seen that on May 25 a strong southwesterly wind blew over the entire region, and the air flow approaching the Crimean Mountains from the southwest split over the sea, flowing around the mountains on both sides. Note that such a homogeneous wind field formed on May 25, after the upwellings had already developed. During the upwelling development on May 23 and 24, the pattern was different (Fig. 2). The wind had a southwesterly direction only over the eastern coast of Crimea; over the western coast, the wind direction was predominantly western, and directly over the Crimean Mountains, northwesterly.

From Fig. 1, *c* it can be seen that near the coast at a depth of 10 m, the water temperature decrease was not limited to the three areas mentioned above, but occurred along the entire coast from Sevastopol to Kerch. Here, a band of cold water about 10 km wide appeared, with a temperature 5–6 °C lower than that of the surrounding waters. Comparison of Fig. 1, *b, c* allows one to conclude that in those coastal sections where the temperature decrease did not manifest itself in the SST field, incomplete upwelling that did not reach the sea surface took place.

Below we consider in more detail the development of two upwelling events near the southern coast of Crimea. Fig. 2 shows the SST and wind speed fields in the Yalta and Feodosia areas for two time periods – before the onset of upwelling and during its development. Based on Fig. 2, *a, b*, it can be concluded that the Yalta upwelling was of the wind-driven type, since it occurred as a result of a sharp intensification of the northwestern wind blowing from the Crimean Mountains toward the sea. According to the modeling results, the surface wind speed in the coastal area on the leeward side of the mountains increased from 6–7 to 12–15 m/s within one day. Although the sea depth in this area is about 60 m and significantly exceeds the Ekman thickness (~15 m), wind-driven upwellings can be observed not only in shallow water but also near steep coasts [7].

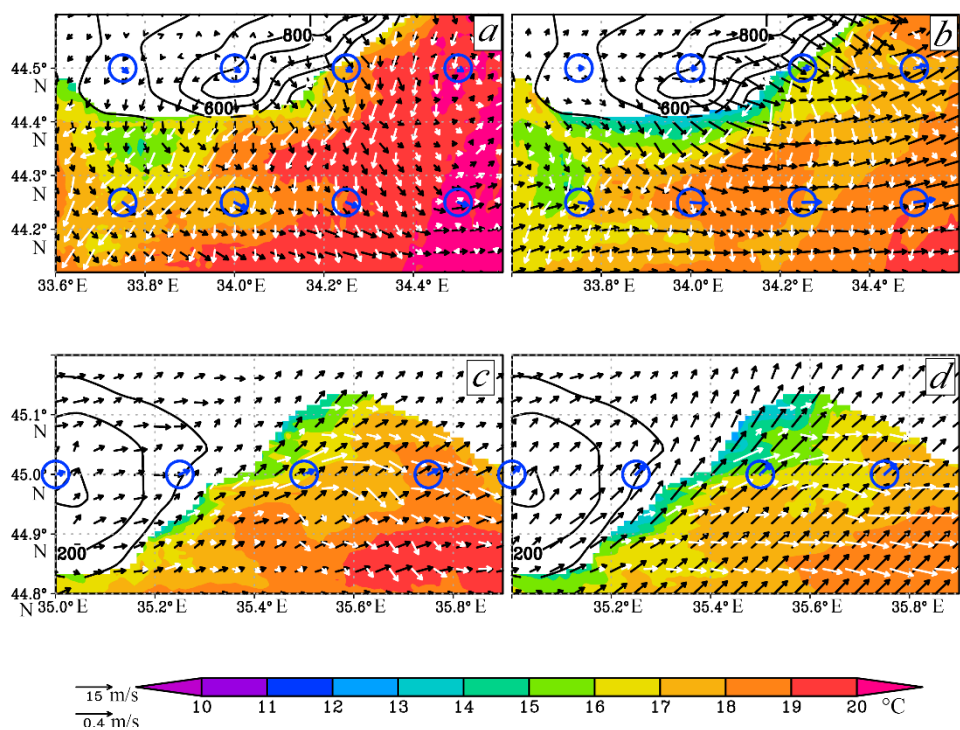


Fig. 2. Sea surface temperature ($^{\circ}\text{C}$) and the near-surface wind field: *a, b* – in the Yalta region at 18:00 on May 23 and May 24, respectively; *c, d* – in the Feodosia region at 18:00 on May 24 and at 06:00 on May 25, 2010. Isolines show topographic height (m), black arrows – near-surface wind velocity, white arrows – surface current velocity (for clarity, the velocity vectors are thinned out); blue arrows in the circles indicate the surface wind velocity based on the ERA5 reanalysis data (the scale is the same as that used for the black arrows)

Fig. 2, *c, d* show that the upwelling near Feodosia occurred as a result of intensification of the alongshore southwesterly wind, i.e., it can be classified as an Ekman-type event. This result agrees with well-known concepts: according to measurements at coastal stations, it has been established that on the southern coast of Crimea, upwelling is favored by winds from western directions (northwest, west, and southwest) [5].

In Fig. 2, to demonstrate how dynamic regionalization improves the quality of atmospheric fields, the surface wind field from the ERA5 reanalysis, which was used as the initial and boundary conditions for the atmospheric block of the coupled model, is also shown. It can be seen that the surface wind speed in the Yalta and Feodosia areas according to ERA5 was noticeably lower than that in the WRF model and did not exceed 8 m/s. The WRF model reproduced not only higher surface wind speeds in the coastal area but also its correct direction (northwestern) in the Yalta region. Thus, dynamic regionalization made it possible

to reproduce small-scale features of surface fields that cannot be obtained by simple interpolation of global reanalysis data onto the ocean model grid.

Fig. 3 gives the vertical structure of the Yalta and Feodosia upwellings on cross sections taken normal to the coastline (the coast is on the right in Fig. 3, *a*, and on the left in Fig. 3, *b*). Arrows show the direction of current velocity in the section plane; for clarity, the vertical velocity component is magnified by 10^3 times.

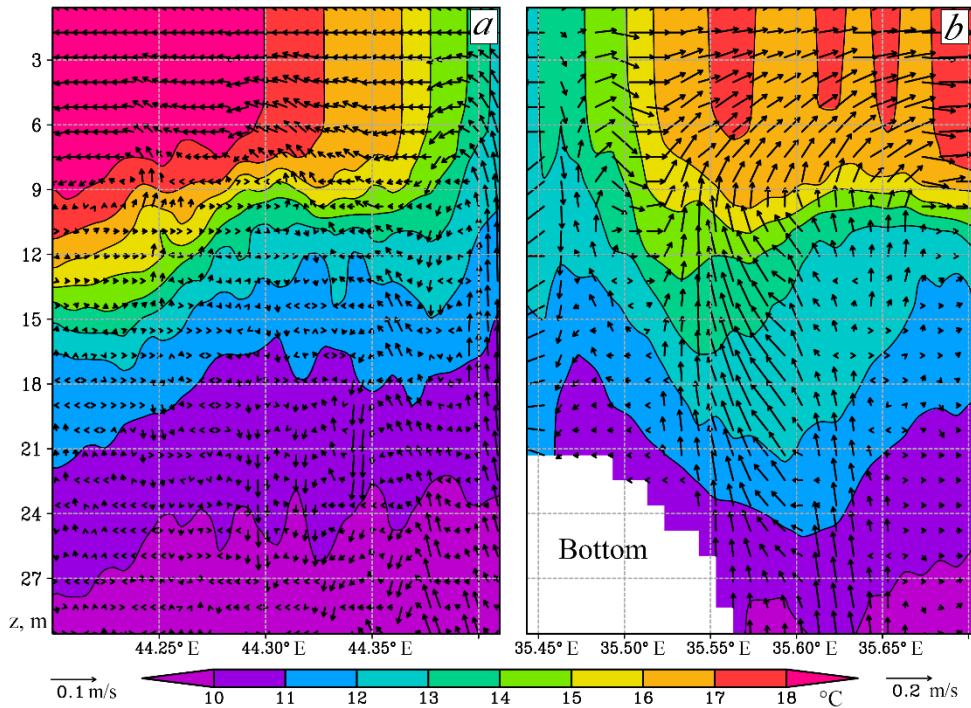


Fig. 3. Water temperature ($^{\circ}\text{C}$) on vertical sections taken normal to the coast: *a* – in the Yalta region at 18:00 on May 24; *b* – in the Feodosia region at 06:00 on May 25. Arrows show the direction of current velocity in the section plane (for clarity, the velocity vertical component is enlarged by 10^3 times). Section locations are shown in Fig. 1, *c*

It can be seen that in the two cross sections, the current in the upper 10 m layer was directed away from the coast. The outflow velocity reached 0.2 m/s in the Yalta upwelling and 0.3 m/s in the Feodosia upwelling. The vertical structure of the currents in Fig. 3, *a, b* differs significantly. In the Yalta upwelling, water uplift was concentrated in close proximity to the coast, in a narrow zone several kilometers wide, and the upward velocity reached 0.05 cm/s. In the Feodosia upwelling, the main uplift occurred at a distance of ~ 15 km from the coast, in the area of the depth drop, where the width of the zone covered by upward motions was ~ 13 km, and the uplift velocity reached 0.03 cm/s.

Fig. 3, *b* shows an interesting feature of the vertical water circulation in the Feodosia upwelling: at depths below 10 m, in the 35.5–35.6 $^{\circ}\text{E}$ zone, a flow

directed toward the coast is clearly distinguished. Without providing illustrations, we note that this alongshore current is a manifestation of a small deep anticyclonic eddy in the Feodosia Gulf, which is clearly visible in the current fields below 10 m. The cross section in Fig. 3, *b* passes through the western periphery of this eddy.

Development of upwelling over time at two points – near Yalta and Feodosia – is shown in Fig. 4. The upper graphs show how the component of the surface wind responsible for upwelling generation changed: for Yalta, this is the component normal to the coast; for Feodosia, it is the alongshore component. The lower graphs show how the depth of the 11°C isotherm and the 18 psu isohaline changed. The points under consideration are the coastal points closest to the cross sections shown in Fig. 1, *c*.

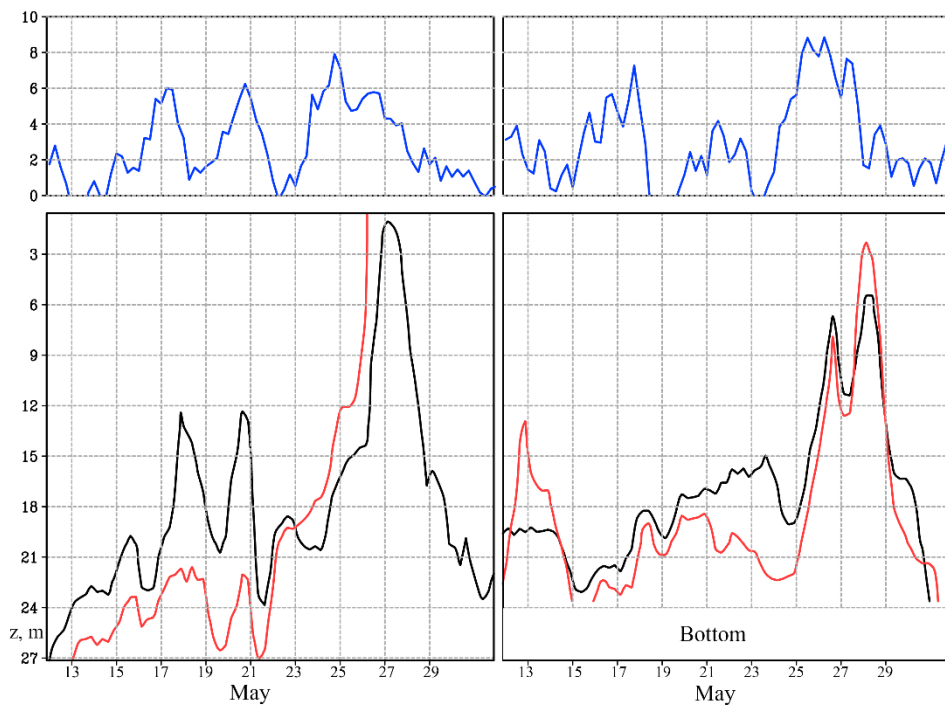


Fig. 4. Changes in wind velocity components (m/s) and isohaline depth (m) at two points: *on the left* – the component directed normal to the coast at point 34.05°E, 44.41°N; *to the right* – the alongshore component at point 35.42°E, 45°N. The black line shows the depth of the 11°C isotherm, and the red line shows the depth of the 18 psu isohaline. For clarity, the graphs are smoothed by a three-point moving average

As can be seen, during May 24–27, the surface wind speed at these points increased sharply, which was accompanied by a rise of both isolines from a depth of ~ 20 m almost to the sea surface. It should be noted that in the Yalta region on May 17 and 21, a short-term wind intensification occurred, although it was not as

significant as on May 24–25. These two episodes were also accompanied by a simultaneous rise of the temperature and salinity isolines (Fig. 4, *a*).

Temporal correlation coefficients between wind speed and the depth of the isolines turned out to be low (< 0.5), indicating a nonlinear relationship between these variables. This is likely because the thermohaline structure of the upper sea layer is influenced by other factors, primarily horizontal advection. Nevertheless, in individual cases, wind intensification at the points under consideration unequivocally led to a decrease in temperature and an increase in salinity in the upper layer.

Without providing illustrations, we note that, according to Copernicus marine reanalysis data, in 2010 the May temperature profiles in the southern coast of Crimea were characterized by a monotonic decrease with depth, since the upper quasi-homogeneous layer had not yet formed. It can be concluded that the SST decrease observed in satellite images at the end of May 2010 is indeed associated with the rise of colder and saltier water from deeper layers as a result of upwelling.

Conclusion

In the present paper, using a coupled ocean-atmosphere model with high spatial resolution (1 km), cases of upwelling development off the Crimean coast in late May 2010 were investigated. It was shown that the model reproduced the areas of reduced sea surface temperature observed in satellite images – near Yalta, near Feodosia, and in the Kerch Strait. It was found that at a depth of 10 m, the water temperature decrease was not limited to these three regions, but occurred along the entire coast from Sevastopol to Kerch.

Based on the modeling results, two upwellings – the Yalta and Feodosia events – were examined in detail. It was established that the Yalta upwelling was of the wind-driven type, since its development was accompanied by an offshore wind. The Feodosia upwelling was of the Ekman type and was caused by southwesterly alongshore winds. The main advantage of dynamic regionalization in coupled modeling has been demonstrated: the atmospheric block of the coupled model reproduced the fine-scale structure of the surface wind field in the Yalta and Feodosia regions, in particular, the intensification of the coastal wind over the sea to significant speeds of 12–15 m/s, which is absent in the atmospheric reanalysis data.

On vertical cross sections taken normal to the coastline, the structure of the two upwellings was studied, and the main difference was noted: in the Yalta upwelling, water uplift was concentrated in a narrow zone directly adjacent to the coast, whereas in the Feodosia upwelling, the main water uplift occurred at some distance from the coast, and the uplift velocity did not reach such high values as in the Yalta upwelling. It was shown that the SST decrease near the indicated areas occurred precisely due to upwelling, since a decrease in surface water temperature was accompanied by a simultaneous increase in salinity and coincided in time with the

intensification of the corresponding coastal wind velocity component (normal to the coast near Yalta and alongshore near Feodosia).

Thus, the performed mesoscale coupled modeling made it possible to reproduce and examine in detail the structure and development of two real upwellings observed off the southern coast of Crimea, which would be difficult to accomplish using only observational data.

REFERENCES

1. Blatov, A.S. and Ivanov, V.A., 1992. [*Hydrology and Hydrodynamics of the Shelf Zone of the Black Sea (on the Example of the Southern Coast of Crimea)*]. Kiev: Naukova Dumka, 224 p. (in Russian).
2. Efimov, V.V., Stanichnyi, S.V., Shokurov, M.V. and Yarovaya, D.A., 2008. Observations of a Quasi-Tropical Cyclone over the Black Sea. *Russian Meteorology and Hydrology*, 33(4), pp. 233-239. <https://doi.org/10.3103/S1068373908040067>
3. Iarovaya, D.A., Efimov, V.V., Barabanov, V.S. and Mizyuk, A.A., 2020. Response of the Black Sea Upper Layer to the Cyclone Passage on September 25–29, 2005. *Russian Meteorology and Hydrology*, 45(10), pp. 701-711. <https://doi.org/10.3103/S1068373920100040>
4. Zatsepin, A.G., Silvestrova, K.P., Kuklev, S.B., Piotoukh, V.B. and Podymov, O.I., 2016. Observations of a Cycle of Intense Coastal Upwelling and Downwelling at the Research Site of the Shirshov Institute of Oceanology in the Black Sea. *Oceanology*, 56(2), pp. 188-199. <https://doi.org/10.1134/S0001437016020211>
5. Lovenkova, E.A. and Polonskii, A.B., 2005. Climatic Characteristics of Upwelling near the Crimean Coast and Their Variability. *Russian Meteorology and Hydrology*, (5), pp. 31-37.
6. Dzhiganshin, G.F., Polonskii, A.B. and Muzyleva, M.A., 2010. Upwelling in the Northwest Part of the Black Sea at the End of the Summer Season and Its Causes. *Physical Oceanography*, 20(4), pp. 281-293. <https://doi.org/10.1007/s11110-010-9084-0>
7. Goryachkin, Y.N. and Ivanov, V.A., 2014. Thermohaline Structure and Dynamics of Waters at the Black Sea Satellite Observation Site. In: V. A. Dulov and V. A. Ivanov, eds., 2014. *Monitoring of the Coastal Zone in the Black Sea Experimental Sub-Satellite Testing Area*. Sevastopol: ECOSI-Gidrofizika, pp. 311-334 (in Russian).
8. Polonskii, A.B. and Muzyleva, M.A., 2016. Modern Spatial-Temporal Variability of Upwelling in the North-Western Black Sea and off the Crimea Coast. *Izvestiya Rossiiskoi Akademii Nauk. Seriya Geograficheskaya*, (4), pp. 96-108. <https://doi.org/10.15356/0373-2444-2016-4-96-108> (in Russian).
9. Goryachkin, Yu.N., 2018. Upwelling nearby the Crimea Western Coast. *Physical Oceanography*, 25(5), pp. 368-379. <https://doi.org/10.22449/1573-160X-2018-4-368-379>
10. Stanichnaya, R.R. and Stanichny, S.V., 2021. Black Sea Upwellings. *Sovremennye Problemy Distantionnogo Zondirovaniya Zemli iz Kosmosa*, 18(4), pp. 195-207. <https://doi.org/10.21046/2070-7401-2021-4-195-207> (in Russian).

11. Shokurova, I.G., Plastun, T.V., Kasianenko, T.E., Stanichnaya, R.R., Krashennnikova, S.B. and Simonova, Yu.V., 2023. Winds Favorable for Upwellings near the Southern Coast of Crimea. *Physical Oceanography*, 30(4), pp. 398-409.
12. Tolstosheev, A.P., Motyzhev, S.V. and Lunev, E.G., 2020. Results of Long-Term Monitoring of the Shelf Water Vertical Thermal Structure at the Black Sea Hydrophysical Polygon of RAS. *Physical Oceanography*, 27(1), pp. 69-80. <https://doi.org/10.22449/1573-160X-2020-1-69-80>
13. Mikhailova, É.N., Polonsky, A.B. and Muzyleva, M.A., 2012. On the Causes of Decrease in the Surface Temperature of Water in the Karkinitsskii Bay of the Black Sea. *Physical Oceanography*, 21(6), pp. 394-400. <https://doi.org/10.1007/s11110-012-9131-0>
14. Osynnyi, V.I. and Shapiro, N.B., 1993. Modeling of Upwelling and Downwelling in the Ocean. *Morskoy Gidrofizicheskiy Zhurnal*, (6), pp. 3-16 (in Russian).
15. Ivanov, V.A., Mikhailova, É.N. and Shapiro, N.B., 2008. Modeling of Wind Upwellings on the Northwest Shelf of the Black Sea near Local Features of the Bottom Topography. *Physical Oceanography*, 18(3), pp. 168-178. <https://doi.org/10.1007/s11110-008-9017-3>
16. Kosnyrev, V.K., Mikhailova, E.N. and Shapiro, N.B., 1996. [Numerical Modeling of Upwelling in the Northwestern Part of the Black Sea]. *Meteorology and Hydrology*, (12), pp. 65-71 (in Russian).
17. Efimov, V.V., Iarovaya, D.A. and Barabanov, V.S., 2023. Numerical Modelling of Upwelling near the South Coast of Crimea on 24–25 September 2013. *Ecological Safety of Coastal and Shelf Zones of Sea*, (1), pp. 6-19.
18. Samson, G., Masson, S., Lengaigne, M., Keerthi, M.G., Vialard, J., Pous, S., Madec, G., Jourdain, N.C., Jullien, S. [et al.], 2014. The NOW Regional Coupled Model: Application to the Tropical Indian Ocean Climate and Tropical Cyclone Activity. *Journal of Advances in Modeling Earth Systems*, 6(3), pp. 700-722. <https://doi.org/10.1002/2014MS000324>
19. Madec, G. and the NEMO team, 2008. *NEMO Ocean Engine*. Note du Pole de Modélisation. Institut Pierre-Simon Laplace (IPSL), France. No. 27, 300 p. <https://doi.org/10.5281/ZENODO.324873920>.
20. Valcke, S., 2013. The OASIS3 Coupler: A European Climate Modelling Community Software. *Geoscientific Model Development*, 6(2), pp. 373-388. <https://doi.org/10.5194/gmd-6-373-2013>

Submitted 05.06.2025; approved after review 03.11.2025;
accepted for publication 28.01.2026.

About the authors:

Daria A. Yarovaya, Leading Researcher, Marine Hydrophysical Institute of RAS (2 Kapitanskaya Str., Sevastopol, 299011, Russian Federation), CSc. (Phys.-Math.), **SPIN-code: 9569-5642**, **ResearcherID: Q-4144-2016**, **ORCID ID: 0000-0003-0949-2040**, **Scopus Author ID: 57205741734**, darik777mhi-ras@mail.ru

Vladimir V. Efimov, Head of the Ocean–Atmosphere Interaction Department, Marine Hydrophysical Institute of RAS (2 Kapitanskaya Str., Sevastopol, 299011, Russian Federation), DSc. (Phys.-Math.), Professor, **SPIN-code: 4902-8602**, **ResearcherID: P-2063-2017**, **Scopus Author ID: 6602381894**, vefim38@mail.ru

Contribution of the co-authors:

Daria A. Yarovaya – formulation of conclusions, conducting calculations, and interpreting modeling results

Vladimir V. Efimov – problem statement, participating in discussions of modeling results, and formulation of conclusions

The authors have read and approved the final manuscript.

The authors declare that they have no conflict of interest.